

# The optical companion to the intermediate mass millisecond pulsar J1439-5501 in the Galactic field<sup>1</sup>

C. Pallanca<sup>2</sup>, B. Lanzoni<sup>2</sup>, E. Dalessandro<sup>2</sup>, F. R. Ferraro<sup>2</sup>, A. Possenti<sup>3</sup>, M. Salaris<sup>4</sup>, M. Burgay<sup>3</sup>.

<sup>2</sup> *Dipartimento di Fisica e Astronomia, Università degli Studi di Bologna, Viale Berti Pichat 6/2, I-40127 Bologna, Italy*

<sup>3</sup> *INAF-Osservatorio Astronomico di Cagliari, località Poggio dei Pini, strada 54, I-09012 Capoterra, Italy*

<sup>4</sup> *Astrophysics Research Institute, Liverpool John Moores University, UK*

May 16, 2013

## ABSTRACT

We present the identification of the companion star to the intermediate mass binary pulsar J1439-5501 obtained by means of ground-based deep images in the  $B$ ,  $V$  and  $I$  bands, acquired with FORS2 mounted at the ESO-VLT. The companion is a massive white dwarf (WD) with  $B = 23.57 \pm 0.02$ ,  $V = 23.21 \pm 0.01$  and  $I = 22.96 \pm 0.01$ , located at only  $\sim 0.05''$  from the pulsar radio position. Comparing the WD location in the  $(B, B - V)$  and  $(V, V - I)$  Color-Magnitude diagrams with theoretical cooling sequences we derived a range of plausible combinations of companion masses ( $1 \lesssim M_{\text{COM}} \lesssim 1.3 M_{\odot}$ ), distances ( $d \lesssim 1200$  pc), radii ( $\lesssim 7.8 \cdot 10^{-3} R_{\odot}$ ) and temperatures ( $T = 31350_{-7400}^{+21500}$ ). From the PSR mass function and the estimated mass range we also constrained the inclination angle  $i \gtrsim 55^{\circ}$  and the pulsar mass ( $M_{\text{PSR}} \lesssim 2.2 M_{\odot}$ ). The comparison between the WD cooling age and the spin down age suggests that the latter is overestimated by a factor of about ten.

*Subject headings:* Stars:Binaries:General, Stars:imaging, Stars:PSR:Individual: PSR J1439-5501, techniques: photometric

---

<sup>1</sup>Based on FORS2 observations collected at the ESO-VLT under program 383.D-0406(A).

## 1. Introduction

According to the canonical recycling scenario, millisecond pulsars (PSRs) form in binary systems containing a neutron star (NS) which is eventually spun up through mass accretion from the evolving companion.

Depending on the companion mass it is possible to classify radio PSRs with evolved companions into three groups: low-, intermediate- and high-mass binary PSRs. In the context of stellar evolution this classification is related to the evolution of stars with low, intermediate and high mass, that evolve to Helium (He), Carbon-Oxygen (CO) or Oxygen-Neon-Magnesium (ONeMg) white dwarfs (WDs), and NS, respectively (Van Kerkwijk & Kulkarni, 1995).

In particular intermediate mass binary PSRs (IMBPs) are thought to be generated from intermediate mass X-ray Binaries (IMXBs), with donor masses typically of  $3 - 6 M_{\odot}$ . Following a supernova explosion, the primary becomes a NS and later the secondary evolves and recycles the PSR through mass transfer, eventually forming a CO- or ONeMg-WD with a He envelope (van den Heuvel 1994; Tauris et al., 2000; Taam et al. 2000). A massive WD can also be left if the companion to the PSR evolved up to the asymptotic giant branch before overflowing its Roche lobe. The latter scenario may lead to more accretion, and thus to a NS spun up to faster periods and with a more strongly reduced magnetic field. The WD might still have a hydrogen envelope. Seventeen candidate IMBP systems are currently known in the Galactic field (Van Kerkwijk et al., 2005; Jacoby et al 2006; Tauris et al., 2012; Burgay et al., 2012).

The optical identification of companion stars to such objects is a crucial point for unveiling their nature and for investigating the formation channels of the binary system (Ferraro et al. 2001, 2003, Cocozza et al. 2008, and Pallanca et al., 2010, 2012). In principle, it allows to accurately estimate the companion mass (see, e.g., Antoniadis et al., 2012) and, in turn, the PSR mass. In that case, binary PSRs can become a unique laboratory for fundamental physics, where the equation of state of matter at nuclear densities can be constrained (see e.g. van Kerkwijk, Breton & Kulkarni 2011) and gravity theories tested (see, e.g., Freire et al., 2012). In case of the identification of a WD companion, its color and magnitude could be used to infer the mass and the cooling age of the WD, which could be compared with the age of the NS to understand the timescale of the magnetic field decay. Note however that only 5 companions to IMBPs have been detected so far in the optical band: PSR B0655+64, PSR J1022+1001, PSR J1528-3146, PSR J1757-5322 and PSR J2145-0750 (van Kerkwijk et al. 1995, 2005; Lundgren et al. 1996a, 1996b; Lohmer et al., 2004 and Jacoby et al. 2006).

In this work we have collected and analyzed a sample of deep multi band images in the

direction of PSR J1439-5501 in the Galactic field, with the aim of identifying the companion star. The plan of the paper is as follows: in Section 2 the known properties of the PSR are listed, while the observations and data analysis are described in Section 3. Results are presented in Section 4 and discussed in Section 5.

## 2. PSR J1439-5501

The binary PSR J1439-5501 was discovered during the first reprocessing (Faulkner et al., 2004) of the data of the Parkes Multibeam Pulsar Survey (Manchester et al., 2001) and its accurate timing parameters were published by Lorimer et al. (2006, hereafter L06). The spin period ( $P \sim 29$  ms) and the surface magnetic field ( $B_s \sim 2.05 \times 10^9$  G) suggest that PSR J1439-5501 belongs to the class of the *mildly* recycled PSRs, i.e. the NS that underwent a relatively short phase of mass accretion from the companion star.

The distance of PSR J1439-5501 can be estimated from its dispersion measure ( $DM \sim 15$  pc cm $^{-3}$ , L06) once a model for the distribution of the electrons in the interstellar medium is adopted. In particular, the TC93 model (Taylor & Cordes 1993) predicts 760 pc, the NE2001 model (Cordes & Lazio 2002) places the PSR at a smaller distance (600 pc), whereas applying the updated Taylor & Cordes model (Schnitzeler, 2012) we obtained a larger distance, of 950 pc. Considering these uncertainties, a possible range<sup>2</sup> for the distance is  $d = 500 - 1200$  pc.

From the observed orbital period,  $P_b = 2.117942520(3)$  d, and the projected semi-major axis of the orbit,  $a_{\text{PSR}} \sin i = 2.947980(3) \times 10^{11}$  cm  $\sim 4.2 R_\odot$  (where  $i$  is the orbital inclination), L06 derived a PSR mass function  $f_{\text{PSR}} = 0.227597 M_\odot$ . This value implies that the companion to PSR J1439-5501 has a mass  $\gtrsim 1 M_\odot$ . In particular, adopting a NS mass  $M_{\text{PSR}} = 1.4 M_\odot$ , the minimum companion mass is  $1.13 M_\odot$  (L06), while assuming the minimum value for radio PSR mass measured so far ( $M_{\text{PSR}} = 1.24 M_\odot$ , Faulkner et al., 2005), the minimum companion mass would be  $1.07 M_\odot$ .

The minimum value for the companion mass leaves 3 options for the nature of this object: an ordinary non degenerate star, a NS, or a very massive CO- or ONe-WD. However a Main Sequence (MS) star with mass as large as  $1.1 M_\odot$  located at the system distance would have magnitude  $R \lesssim 15$ . The inspection of archive images (ESO-DSS) shows that no such bright stars are observed close to the nominal position of PSR J1439-5501. On the other hand the very small observed eccentricity of the orbit ( $e = 5 \times 10^{-5}$ ; L06) strongly

---

<sup>2</sup> However, for our detailed analysis below, the range of available WD models forces us to use a slightly reduced range,  $d = 600 - 1200$  pc (but see section 4).

argues against the hypothesis that the companion is a NS. In fact, in this case it should be the remnant of the massive star that first recycled PSR J1439-5501, and then exploded in a supernova. This should have probably left a significant eccentricity in the system, at odds with the observations.

In view of the considerations above, the companion is most likely a massive WD, and the system J1439-5501 belongs to the growing class of the so-called IMBPs (Camilo et al. 1996). Given its orbital and spin period, the favored scenario, among those discussed by Tauris et al. (2012), is that the system was originated from the evolution of an IMXB with an asymptotic giant branch companion, through a common envelope phase.

### 3. Observations and data analysis

The photometric data set used for this work consists of a series of ground-based optical images acquired with the FOcal Reducer/low dispersion Spectrograph 2 (FORS2) mounted at the ESO-VLT. We performed the observations in the *Standard Resolution mode*, with a pixel scale of  $0.126''/pixel$  (adopting a binning of  $1 \times 1$  pixels) and a field of view (FOV) of  $6'.8 \times 6'.8$ . All the brightest stars in the FOV have been covered with occulting masks in order to avoid artifacts produced by objects exceeding the detector saturation limit in long exposures, which would have significantly hampered the search for faint objects.

A total of 39 deep images in the  $B_{HIGH}$ ,  $V_{HIGH}$  and  $I_{BESS}$  bands were collected during five nights in May 2009, under program 383.D – 0406(A) (PI: B. Lanzoni). Since the goal of this work is to identify the companion to PSR J1439-5501, only the chip containing the region around the nominal position of the PSR has been analyzed.

By following standard reduction procedures, we corrected the raw images for bias and flat-field. In particular, in order to obtain high-quality master-bias and master-flat images, we combined a large number of BIAS and FLAT images obtained during the observation period by using the tasks `zerocombine` and `flatcombine` in the IRAF<sup>3</sup> package CCDRED. The calibration files thus obtained have been applied to the raw images by using the dedicated task `ccdproc`.

We carried out the photometric analysis by using DAOPHOT (Stetson 1987, 1994). The point spread function (PSF) has been modeled in each image by using about 100 bright,

---

<sup>3</sup> IRAF is distributed by the National Optical Astronomy Observatory, which is operated by the Association of Universities for Research in Astronomy, Inc., under the cooperative agreement with the National Science Foundation.

isolated and not saturated stars. The PSF model and its parameters have been chosen using the DAOPHOT PSF routine on the basis of a  $\chi^2$  test. A Moffat function (Moffat 1969) turned out to provide the best fit in all images.

Since our purpose is to detect the faintest stars in the field, we first combined all the available images obtaining a master frame. Then we imposed a detection limit of  $3\sigma$ , where  $\sigma$  is the standard deviation of the measured background. By using the DAOPHOT FIND routine, we thus obtained a master list of objects. Finally, the star positions in this master frame has been adopted as reference to force the object detection and PSF fitting in each single image, by using `allframe` (Stetson 1987, 1994). This procedure also allowed us to achieve an improved determination of the star centroids and a better reconstruction of the star intensity profiles. At the end of the reduction procedure we obtained a catalog of about 4000 sources (see Table 1 for a small sub-sample of the catalog).

*Photometric calibration:* We selected ten bright and isolated stars and, for each of them, we performed aperture photometry with different radii ( $r$ ) and we compared these magnitudes with those obtained with the PSF fitting. The mean value of the differences between PSF and aperture magnitudes has been found to be constant for  $r \geq 13$  pixels. Thus we used the value at  $r = 13$  pixels as aperture correction to be applied to all the stars in our catalog. For a straightforward comparison with theoretical models, we decided to calibrate the instrumental magnitudes ( $b, v, i$ ) to the standard Johnson photometric system ( $B, V, I$ ). To this aim, we first derived the calibration equations for ten standard stars in the field PG1323 (Stetson 2000), which has been observed with FORS2 during the observing run under photometric conditions. To analyze the standard star field we used the DAOPHOT PHOT task and we performed aperture photometry with the same radius used for the aperture correction. We then compared the obtained magnitudes with the standard Stetson catalog available on the CADC web site<sup>4</sup>. The comparison shows a clear dependence on color. Hence we performed a linear fit in order to derive the trend as a function of the color ( $v - i$ ) in case of  $V$  and  $I$  bands and of the  $(b - v)$  for the  $B$ -band. The resulting calibration equations are  $B = b + 0.126(b - v) + 27.16$ ,  $V = v + 0.051(v - i) + 27.53$  and  $I = i - 0.002(v - i) + 26.95$  and the final uncertainties on the calibrated magnitudes are  $\pm 0.016$ ,  $\pm 0.004$  and  $\pm 0.010$  for  $B, V$  and  $I$ , respectively. We neglected the dependence on airmass since all exposures were taken at similar values.

*Astrometry:* Since in the Galactic field proper motions may not be negligible, we used as astrometric reference stars the objects in the catalog PPMXL (Roeser, 2010), where the proper motion of each star is listed. Since the number of objects in common with our

---

<sup>4</sup><http://cadwww.dao.nrc.ca/community/STETSON/standards/>

dataset is large enough (126 stars), we could derive appropriate coordinate transformations. As first step of the procedure we derived the position of the astrometric stars at the epoch of the observations. Then we registered the pixel coordinates of the reference image onto the absolute coordinate system through the cross-correlation of the primary astrometric standards in common with our catalog, by using CataXcorr<sup>5</sup>. The root mean square of the adopted transformations is  $\sim 0.3''$  in right ascension ( $\alpha$ ) and  $\sim 0.2''$  in declination ( $\delta$ ), while the typical uncertainty of the PPMXL stars in this field is  $\sim 0.1''$ . These quantities give an accuracy of  $\sim 0.11''$  for our astrometric solution.

#### 4. The identification of the companion to PSR J1439-5501

In order to identify the companion to PSR J1439-5501 we focused our attention to any object located close to the PSR nominal position, as derived from the timing solution in the radio band:  $\alpha_{2000} = 14^{\text{h}}39^{\text{m}}39^{\text{s}}.742(1)$  and  $\delta_{2000} = -55^{\circ}01'23''.62(2)$  at the reference epoch MJD=53200 (L06). No determination of the PSR proper motion was reported in L06. However, assuming a conservative transverse velocity of  $\sim 100 \text{ km s}^{-1}$  (Hobbs et al., 2005) the expected total positional shift would be  $\sim 0.15''$  (for the system distance) over the  $\sim 5 \text{ yr}$  interval between the reference epoch of the radio ephemeris and the date of optical observations. Therefore, the offset between the position of the system J1439-5001 in the optical images and the coordinates given by L06 would be at most of the order of the astrometric solution accuracy. We also note that follow-up timing observations of the system provide additional support to a safe use of the coordinates reported in L06: in fact these observations indicate a transverse velocity for PSR J1439-5501 well below  $100 \text{ km s}^{-1}$  (Burgay, private communication).

A visual inspection of the deep images shows that there is a star located at only  $0.05''$  from the nominal position of PSR J1439-5501 (see Figure 1). Moreover, no other star in our catalog is found within an error circle centered on the PSR position and having a radius of several times the aforementioned uncertainty in the astrometric solution.

A comparison among the  $I$ ,  $V$  and  $B$  images shown in Figure 1 clearly suggests that this star has a color bluer than most of others objects in the field. This feature is confirmed by the inspection of the Color-Magnitude Diagrams (CMDs), where the star is located on the left side of the bulk of the detected stars, in a region compatible with WD cooling sequences

---

<sup>5</sup>CataXcorr is a code aimed at cross-correlating catalogs and finding astrometric solutions, developed by P. Montegriffo at INAF - Osservatorio Astronomico di Bologna. This package has been successfully used in a large number of papers of our group in the past 10 years.

(see Figure 2). This is in nice agreement with the scenario proposed for the evolution of the system J1439-5501 discussed in Section 2. The probability that any star in our catalog falls at the PSR position by chance coincidence is low ( $\sim 2\%$ ), and it further reduces to  $\sim 0.003\%$  if only WDs are considered. The combination of all these pieces of evidence strongly suggests that the detected star is the companion to PSR J1439-5501.

In principle, companions to MSPs can show optical variability, due to irradiation by the PSR or by rotational modulation, as observed in the case of PSR 0655+64 (Van Kerkwijk et al., 1995 & Van Kerkwijk, 1997). By comparing the flux of the PSR intercepted by the WD with the WD flux we estimated that the flux enhancement due to re-heating is negligible. Unfortunately we could not check if the system shows any variability due to rotation since the largest available number of observations is in the  $I$  band, in which the object is very faint (see Figure 1), while on the  $B$  and  $V$  bands the orbital sampling is very poor and prevents any study of variability. Hence with the available data it is not possible to set a definitive conclusion about the presence of magnitude modulations. Therefore, in order to detect possible variability, and eventually study its nature, future phase resolved observations are required.

With the aim of deriving mass and age of the companion, we compared its position in the CMDs ( $B = 23.57 \pm 0.02$ ,  $V = 23.21 \pm 0.01$  and  $I = 22.96 \pm 0.01$ ) with a set of theoretical CO- and ONe-WD cooling sequences of different masses (BaSTI database, Salaris et al., 2010; Althaus et al., 2007). In order to make consistent the ONe-WD models with CO-WD cooling sequences we applied to the formers the same color transformations used for the latters. As a first step, we calculated the extinction coefficient  $E(B - V)$  by generating the Color-Color (CC) diagram ( $V - I, B - V$ ), where the dependence on distance disappears. In particular, we compared the observed distribution of MS stars (within  $30''$  from PSR J1439-5501) with the locus of theoretical models, with solar metallicity and different ages, typical of the Galactic field population. Different reddening values, ranging between 0.4 and 0.7 with steps of  $\delta E(B - V) = 0.001$ , have been iteratively applied to theoretical models. By performing a  $\chi^2$  test, we obtained that the best-fit value<sup>6</sup> is  $E(B - V) \sim 0.54_{-0.05}^{+0.06}$  (see Figure 3).

In the following we will adopt  $E(B - V) = 0.54$ , keeping in mind that any estimate of the WD mass, distance and derived quantities depends on the  $E(B - V)$  value. As can be seen from Figure 3, if  $E(B - V) = 0.54$  is assumed, the colors of the companion nicely

---

<sup>6</sup>The uncertainties on  $E(B - V)$  have been estimated by accounting for the magnitude errors of the observed population.

match the theoretical sequences for WDs<sup>7</sup>.

By taking into account the absorption coefficients properly calculated for the effective wavelengths of the filters (Cardelli et al., 1989), we derived the unabsorbed colors  $(V - I)_0 = -0.32_{-0.07}^{+0.09}$  and  $(B - V)_0 = -0.21_{-0.07}^{+0.09}$ , from which we estimated a temperature  $T = 31350_{-7400}^{+21500}$ .

By using the derived value of the reddening and the adopted range of distances (600 – 1200 pc; see section 2) we placed the WD cooling sequences for masses of 0.6 and 1.0  $M_\odot$  selected from the BaSTI database (Salaris et al. 2010) in the  $(V, V - I)$  and the  $(B, B - V)$  CMDs. As can be seen from Figure 2, the companion is clearly not compatible with low mass WDs, while it appears to be slightly more massive than 1.0  $M_\odot$ .

In order to better constrain the mass of the companion we needed a tight sampling in mass. Starting from the available tracks for CO- and ONe-WDs in the mass range 1–1.25  $M_\odot$  (Salaris et al., 2010; Althaus 2007) and assuming as a first approximation a linear relation between magnitude, color and mass in such a small range, we derived cooling sequences between 1.0 and 1.25  $M_\odot$  at regular steps. By using the same linear relation we obtained tracks up to 1.3  $M_\odot$ . For each mass ( $m$ ) step we varied the PSR distance ( $d$ ) in the range 600–1200 pc, and we calculated the difference ( $\Delta$  expressed in magnitude units) between the observed location of the companion in the CMD and its perpendicular projection onto the cooling sequence. We applied this method in both the  $(B, B - V)$  and  $(V, V - I)$  CMDs, thus obtaining  $\Delta_1$  and  $\Delta_2$ , respectively, for any  $m$ - $d$  pair. For each value of  $m$  we then selected the value of  $d$  which minimizes the sum of  $|\Delta_1| + |\Delta_2|$  and we associated a confidence value to each  $m$ - $d$  pair. In each CMD the confidence value is calculated as  $|\Delta|$  normalized to the photometric combined error  $\sqrt{(e_{COL}^2 + e_{MAG}^2)}$  of the star. In this way, the smaller is the confidence value, the larger is the probability associated to that configuration. In particular, a confidence value  $\leq 1$  means that the cooling sequence and the observed position are in agreement within the photometric errors. The resulting confidence value, when information from both CMDs is combined, is the sum of the confidence values derived from the two CMDs. The resulting distribution of confidence values in the  $m$ - $d$  plane is plotted in Figure 4. All the  $m$ - $d$  couples for which the confidence value is  $\leq 1$  in both CMDs, have been selected as plausible combinations of  $m$  and  $d$  for the companion (they are encircled by the white contour in Figure 4).

From this analysis we find that, for the considered upper limit to the distance ( $d = 1200$  pc),  $M_{COM} \gtrsim 1M_\odot$  (see Figure 4). Considering the constraint on the minimum companion

---

<sup>7</sup> Note that the theoretical models shown in Figure 3 are for 1.2  $M_\odot$  WDs. However the dependence of the WD cooling sequences on mass is negligible in the  $(V - I, B - V)$  CC Diagram (Bergeron et al., 1995).



mass from the PSR mass function ( $M_{\text{COM}} > 1.07M_{\odot}$ ), we can safely confirm that  $d \leq 1200$  pc. At small distances, the analysis is limited by the availability of WD models (see above). However, the adopted upper limit for the mass in our analysis ( $M_{\text{COM}} = 1.3M_{\odot}$ ) likely does not affect the results, even if we cannot definitely rule out a more massive companion in the range  $1.3 < M_{\text{COM}} < M_{\text{CH}}$ , where  $M_{\text{CH}} = 1.44M_{\odot}$  is the Chandrasekhar mass limit for a WD (Chandrasekhar, 1935). If the companion is a CO-WD it would have a mass  $1.07 \lesssim M_{\text{COM}} \lesssim 1.3 M_{\odot}$ , located at a distance  $710 \lesssim d \lesssim 1200$  pc (see Figure 4), which imply a radius in the range  $4.5 - 7.7 \cdot 10^{-3} R_{\odot}$ . In case of ONe-WDs models, we found  $m$ - $d$  configurations as probable as those obtained for CO-WDs. Hence, the companion to PSR J1439-5501 could also be a ONe-WD with mass  $1.07 \lesssim M_{\text{COM}} \lesssim 1.3 M_{\odot}$ , radius in the range  $4.0 - 7.8 \cdot 10^{-3} R_{\odot}$  and located at distance  $640 \lesssim d \lesssim 1200$  pc. Note that, because of the larger molecular weight of the ONe-WD with respect to the CO-WDs, the former have a smaller radius and hence, for a fixed mass, to fit the observed properties they should be located closer than CO-WDs.

## 5. Discussion and conclusions

From the PSR mass function  $f_{\text{PSR}} = 0.227597 M_{\odot}$  (L06) and the range of permitted companion masses and radii derived in the previous Section, we constrained  $M_{\text{PSR}}$  and the inclination of the system, as summarized in Figure 5. First of all, given the relatively large orbital separation  $\sim 9.5 R_{\odot}$  and the small radius of the companion, the absence of observed eclipses of the radio signal along the orbit only constraints  $i < 89.4^{\circ}$ . The observation of the Shapiro delay effect could allow one to impose further constraints on the inclination. Unfortunately, the quality of the available radio timing (with a non uniform orbital coverage especially close to superior conjunction, where the effect of the Shapiro delay is maximum) does not allow at the moment to extract a constraining determination of the Shapiro delay parameters in this system. However, simulations show that, even with the few times of arrival that we have around orbital phase 0.25, a signature of an almost edge-on orbit would be detectable. We can hence constrain the inclination angle to be  $\lesssim 87^{\circ}$ . Simulating a data set with monthly observations and the current instrumentation, a determination of the Shapiro delay would take from  $\sim 1$  to 3 decades, depending on the inclination of the source (in the range from 60 to 85 degrees). Instead, a lower limit of  $54.8^{\circ}$  for  $i$  results from the assumption that  $M_{\text{COM}} = M_{\text{CH}}$  and that the PSR has a mass larger than  $1.24M_{\odot}$  (see Section 1). Moreover, by adopting  $M_{\text{COM}} = M_{\text{CH}}$  and  $i = 87^{\circ}$ , an upper limit of  $2.18 M_{\odot}$  can be inferred for the PSR mass.

Of all the CO-WD companions to IMBPs identified so far, the companion to PSR

J1439-5501 is one of the few with a mass estimate. Moreover, comparing its estimated mass with the median of companion masses of previously identified CO-WDs (see Tauris et al. 2012), it turns out to be among the most massive.

Although the cooling age of a WD suffers from uncertainties, it is the only reliable age indicator of a PSR binary system (Tauris, 2012). Hence, the optical identification of a WD companion to a binary millisecond pulsar and its cooling age estimate are of crucial importance to constrain the spin-down theory and understand how the characteristics and the age of a PSR are related. Kulkarni (1986) proposed for the first time a comparison between these two ages, finding a quite good agreement. However, there is an increasing body of evidence (see e.g. Tauris et al., 2012) that the spin-down age is a very poor measure of the time that a recycled PSR spent since the completion of mass transfer. In fact, in several PSRs, WDs are observed to be both older and younger than the millisecond pulsar (Hansen & Phinney, 1998a,b). However, in most cases the NS seems to be older than the WD because the standard spin-down model may overestimate the PSR age (Jacoby et al., 2006). For the parameters inferred above, the cooling age of the companion is in the range  $0.1 \lesssim t_{cool} \lesssim 0.2$  Gyr and  $0.1 \lesssim t_{cool} \lesssim 0.4$  Gyr for CO- and ONe-WD respectively (and up to  $0.4 - 0.5$  Gyr for the minimum reddening configuration) and it is several times smaller than its estimated spin-down age ( $3.2 - 4.5$  Gyr; Kiziltan and Thorsett, 2010). This discrepancy is not surprising. In fact the characteristic age for PSRs in the millisecond regime could not be a proper estimate of the PSR ages, since the hypothesis that  $P_0$  is negligible with respect to the current  $P$  is not applicable to recycled PSRs. Such a scenario is in agreement with the results of simulations of an evolved synthetic population of MSPs (Kiziltan and Thorsett, 2010), which shows that the characteristic ages could either over- or under-estimate the true age of MSPs by more than a factor of ten. Hence, we stress how the identification of the companion and its age estimate (e.g. from the cooling sequences for WD companions) could be a powerful tool to derive the true age of a recycled PSR.

While a spectroscopic analysis, both for the radial velocity curve and the chemical analysis, is hardly feasible with the current generation of instrumentation, a photometric follow-up could provide plenty of useful information. In particular, phase resolved datasets could lead to the possibility of revealing any optical variability of the companion, while multi-band photometry could allow to better estimate the reddening and, by applying the same method used in this paper, to better constrain the mass and the distance of the companion.

## 6. Acknowledgement

We thank the Referee Van Kerkwijk for the careful reading of the manuscript and the useful comments. This research is part of the project Cosmic-Lab funded by the European Research Council (under contract ERC-2010-AdG-267675).

## REFERENCES

- Althaus, L. G., García-Berro, E., Isern, J., Córscico, A. H., & Rohrmann, R. D. 2007, *A&A*, 465, 249
- Antoniadis, J., van Kerkwijk, M. H., Koester, D., et al. 2012, *MNRAS*, 423, 3316
- Bergeron, P., Wesemael, F., & Beauchamp, A. 1995, *PASP*, 107, 1047
- Burgay, M., Keith, M. J., Lorimer, D. R., et al. 2012, *MNRAS*, 289
- Camilo, F., Nice, D. J., Shrauner, J. A., & Taylor, J. H. 1996, *ApJ*, 469, 819
- Cardelli, J. A., Clayton, G. C., & Mathis, J. S. 1989, *ApJ*, 345, 245
- Chandrasekhar, S. 1935, *MNRAS*, 95, 207
- Cocozza, G., Ferraro, F. R., Possenti, A., et al. 2008, *ApJ*, 679, L105
- Cordes, J. M., & Lazio, T. J. W. 2002, *arXiv:astro-ph/0207156*
- Faulkner, A. J., Stairs, I. H., Kramer, M., et al. 2004, *MNRAS*, 355, 147
- Faulkner, A. J., Kramer, M., Lyne, A. G., et al. 2005, *ApJ*, 618, L119
- Ferraro, F. R., Possenti, A., D’Amico, N., & Sabbi, E. 2001, *ApJ*, 561, L93
- Ferraro, F. R., Possenti, A., Sabbi, E., & D’Amico, N. 2003, *ApJ*, 596, L211
- Freire, P. C. C., Wex, N., Esposito-Farèse, G., et al. 2012, *MNRAS*, 423, 3328
- Hansen, B. M. S., & Phinney, E. S. 1998, *MNRAS*, 294, 569
- Hansen, B. M. S., & Phinney, E. S. 1998, *MNRAS*, 294, 557
- Hobbs, G., Lorimer, D. R., Lyne, A. G., & Kramer, M. 2005, *MNRAS*, 360, 974

- Jacoby, B. A., Chakrabarty, D., van Kerkwijk, M. H., Kulkarni, S. R., & Kaplan, D. L. 2006, *ApJ*, 640, L183
- Kiziltan, B., & Thorsett, S. E. 2010, *ApJ*, 715, 335
- Kulkarni, S. R. 1986, *ApJ*, 306, L85
- Löhmer, O., Kramer, M., Driebe, T., et al. 2004, *A&A*, 426, 631
- Lorimer, D. R., Faulkner, A. J., Lyne, A. G., et al. 2006, *MNRAS*, 372, 777
- Lundgren, S. C., Ergma, E., & Cordes, J. M. 1996a, *IAU Colloq. 160: Pulsars: Problems and Progress*, 105, 521
- Lundgren, S. C., Cordes, J. M., Foster, R. S., Wolszczan, A., & Camilo, F. 1996b, *ApJ*, 458, L33
- Manchester, R. N., Lyne, A. G., Camilo, F., et al. 2001, *MNRAS*, 328, 17
- Moffat, A. F. J. 1969, *A&A*, 3, 455
- Pallanca, C., Dalessandro, E., Ferraro, F. R., et al. 2010, *ApJ*, 725, 1165
- Pallanca, C., Mignani, R. P., Dalessandro, E., et al. 2012, *ApJ*, 755, 180
- Roeser, S., Demleitner, M., & Schilbach, E. 2010, *AJ*, 139, 2440
- Salaris, M., Cassisi, S., Pietrinferni, A., Kowalski, P. M., & Isern, J. 2010, *ApJ*, 716, 1241
- Schnitzeler, D. H. F. M. 2012, *MNRAS*, 427, 664
- Stetson, P. B. 1987, *PASP*, 99, 191
- Stetson, P. B. 1994, *Calibrating Hubble Space Telescope*, 89
- Stetson, P. B. 2000, *PASP*, 112, 925
- Taam, R. E., King, A. R., & Ritter, H. 2000, *ApJ*, 541, 329
- Tauris, T. M., van den Heuvel, E. P. J., & Savonije, G. J. 2000, *ApJ*, 530, L93
- Tauris, T. M. 2012, *Science*, 335, 561
- Tauris, T. M., Langer, N., & Kramer, M. 2012, *MNRAS*, 425, 1601
- Taylor, J. H., & Cordes, J. M. 1993, *ApJ*, 411, 674

- van den Heuvel, E. P. J. 1994, *A&A*, 291, L39
- van Kerkwijk, M. H., & Kulkarni, S. R. 1995, *ApJ*, 454, L141
- van Kerkwijk, M. H. 1997, *White dwarfs*, 214, 383
- van Kerkwijk, M. H., & Kulkarni, S. R. 1999, *ApJ*, 516, L25
- van Kerkwijk, M. H., Bassa, C. G., Jacoby, B. A., & Jonker, P. G. 2005, *Binary Radio Pulsars*, 328, 357
- van Kerkwijk, M. H., Breton, R. P., & Kulkarni, S. R. 2011, *ApJ*, 728, 95

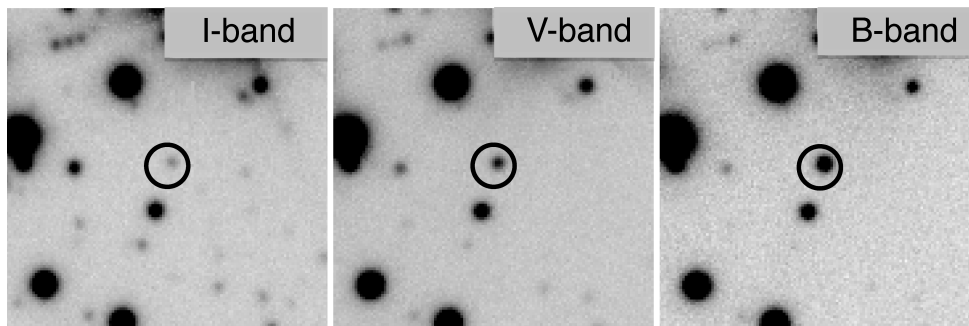


Fig. 1.— From left to right,  $15'' \times 15''$  maps in the  $I_{BESS}$ ,  $V_{HIGH}$  and  $B_{HIGH}$  bands around the PSR nominal position. The black circles are centered on PSR J1439-5501 and have a radius of  $1''$ .

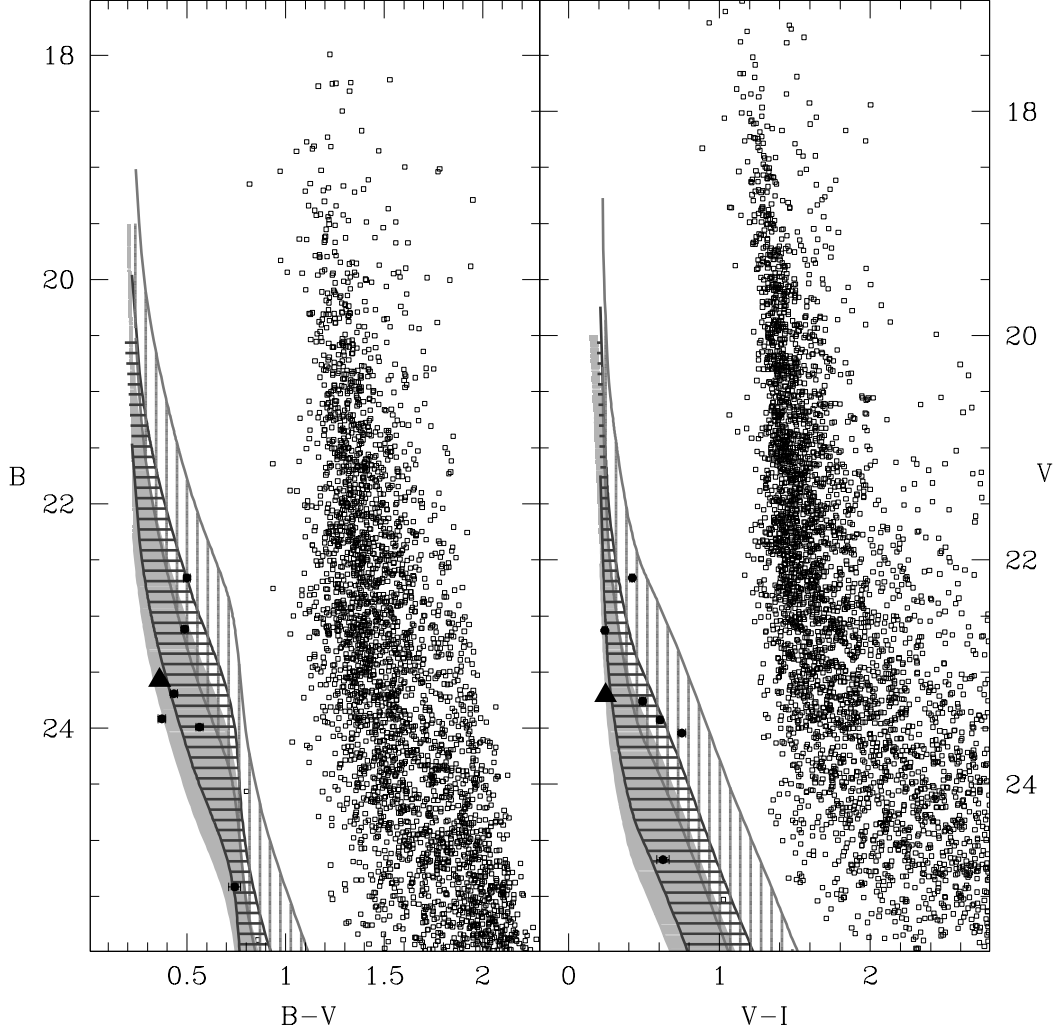


Fig. 2.—  $(B, B - V)$  and  $(V, V - I)$  Color-Magnitude Diagrams for the companion to PSR J1439-5501 (black triangle) and for all the other objects observed in the detector FOV. The companion is located at  $B = 23.57 \pm 0.02$ ,  $V = 23.21 \pm 0.01$  and  $I = 22.96 \pm 0.02$ , corresponding to the region of WD cooling sequences. The vertically and the horizontally hatched bands correspond to the CO-WD cooling sequences, respectively, for  $0.6$  and  $1.0 M_{\odot}$ , in a range of distances between  $600$  and  $1200$  pc (BaSTI database; Salaris et al., 2010), while the shaded light gray strip marks, in the same distance range, the location of a  $1.0 M_{\odot}$  ONe-WD (Althaus et al., 2007).

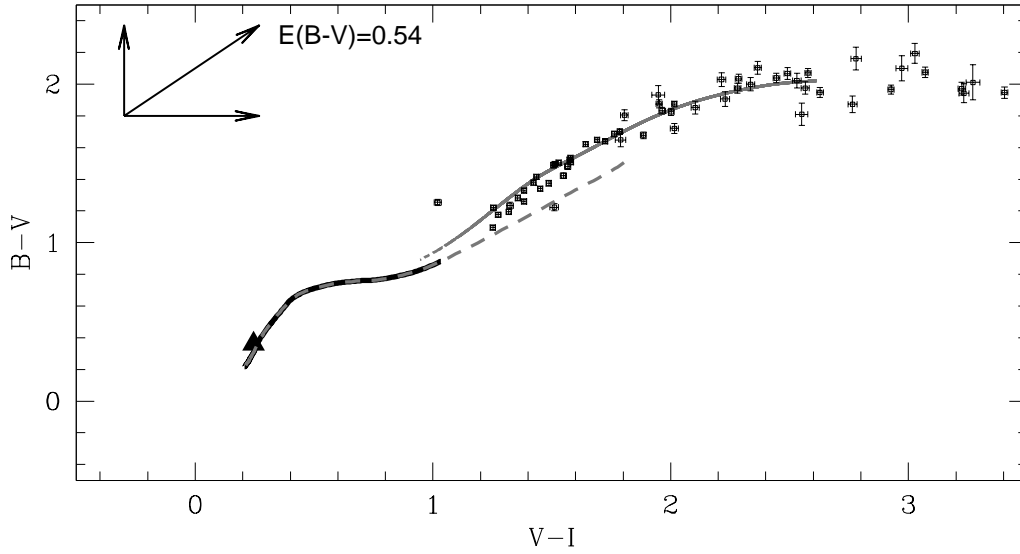


Fig. 3.—  $(V - I, B - V)$  Color-Color diagram for all stars (open squares) within  $30''$  from PSR J1439-5501. The companion is highlighted with a large black triangle. The gray solid region marks the location of MS populations having solar metallicity and different ages, consistent with those observed in the Galactic field. The black solid and gray dashed lines correspond to the cooling sequences for  $1.2M_{\odot}$  CO- and ONe-WDs, respectively. A color excess  $E(B - V) = 0.54$  is applied to the models (arrows mark the entity and direction of the applied reddening).



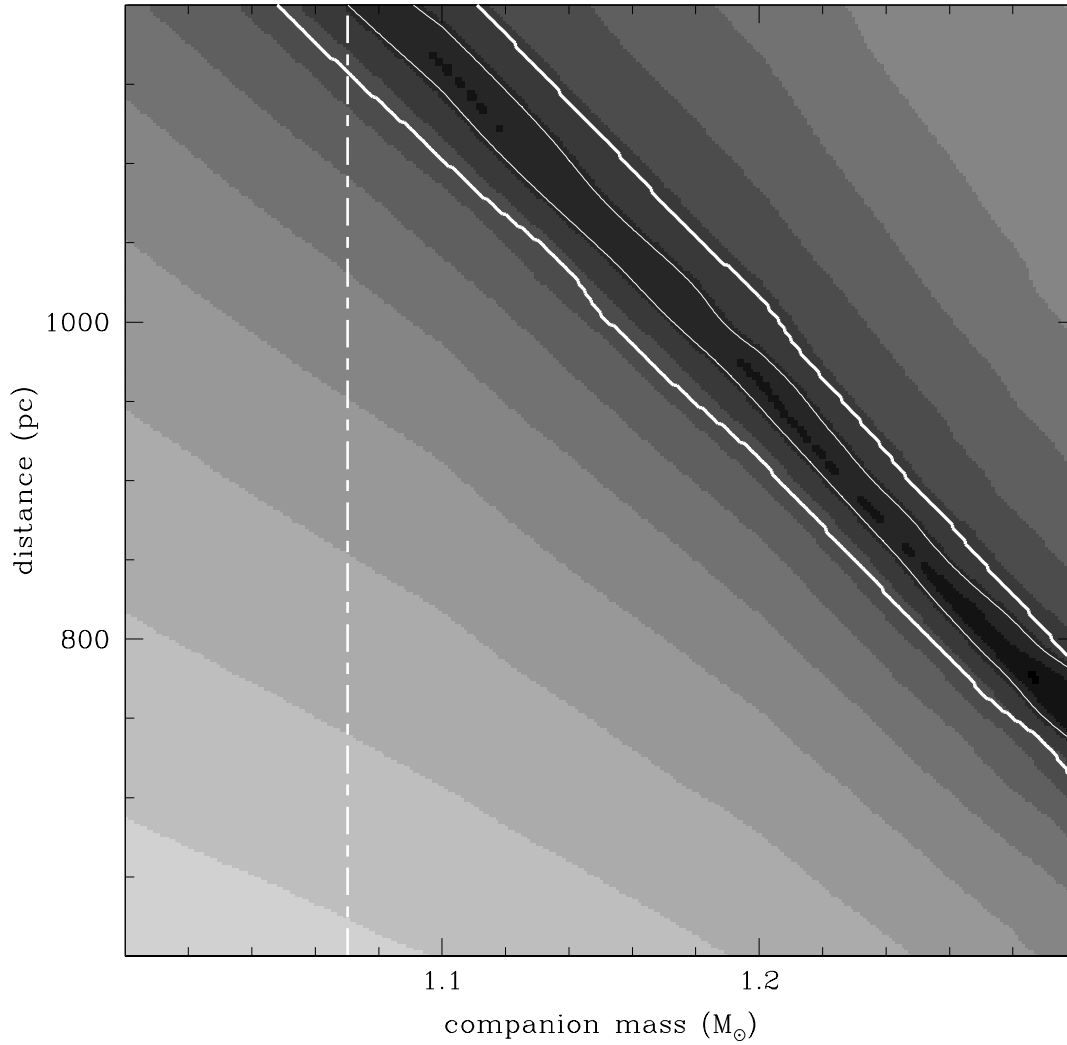


Fig. 4.— Distribution of probabilities for CO-WDs in the plane of companion mass ( $m$ ) and system distance ( $d$ ). Darker regions mean more probable configurations. The thick white contour marks the region occupied by couples  $m$ - $d$  providing confidence values  $\leq 1$  in both CMDs, the thin white line encircles the configurations with confidence value  $\leq 1$ .

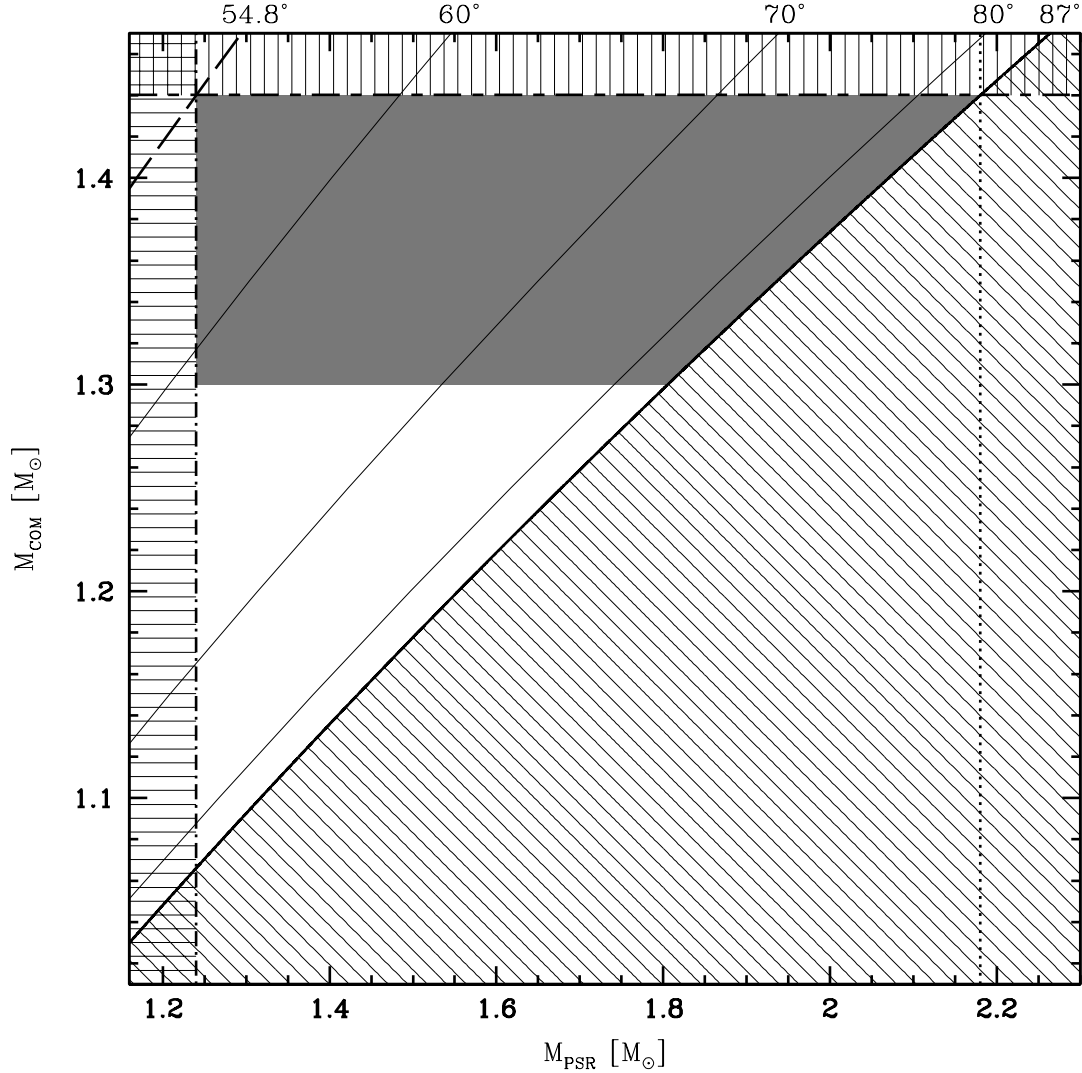


Fig. 5.— Companion mass as a function of the PSR mass. Solid lines indicate constant orbital inclinations from the PSR mass function. In particular the thick solid line marks the limit of  $i_{\max} = 87^\circ$ . The short-long dashed line marks the physical limit  $M_{\text{CH}} = 1.44M_\odot$  for the WD mass. The dot dashed line marks the minimum limit  $M_{\text{NS,min}} = 1.24M_\odot$  ever measured for a radio pulsar mass. The hatched regions are excluded because of the combination of the physical limits above. The dotted line indicates the upper limit to the PSR mass  $M_{\text{PSR}} < 2.18$  derived assuming  $M_{\text{COM}} = M_{\text{CH}}$  and  $i = i_{\max}$ ; while the long dashed line indicates the lower limit to the inclination angle  $i > 54.8^\circ$  calculated assuming  $M_{\text{COM}} = M_{\text{CH}}$  and  $M_{\text{PSR}} = M_{\text{NS,min}}$ . The white region marks the investigated range of WD masses by comparison between optical photometry and theoretical models. Note that we could not extend the analysis to companions more massive than  $1.3M_\odot$  (gray region) because models for WD with larger masses are not available.

ID	R.A. (J2000)	Dec. (J2000)	$B$	$eB$	$V$	$eV$	$I$	$eI$
1★	14:39:39.746	-55:01:23.66	23.57	0.02	23.21	0.01	22.96	0.02
2	14:39:43.006	-55:00:47.58	22.24	0.02	21.00	0.01	19.66	0.01
3	14:39:41.277	-55:01:10.81	22.16	0.02	20.51	0.01	18.82	0.01
4	14:39:40.619	-55:01:14.66	21.46	0.02	19.96	0.01	18.43	0.01
5	14:39:40.234	-55:00:55.79	22.70	0.02	21.21	0.01	19.71	0.01
6	14:39:38.596	-55:00:40.84	21.34	0.02	19.98	0.01	18.60	0.01
7	14:39:38.068	-55:00:45.54	23.09	0.02	21.75	0.01	20.32	0.01
8	14:39:37.287	-55:00:50.09	23.53	0.02	21.98	0.01	20.28	0.01
9	14:39:36.626	-55:01:24.52	21.39	0.02	20.20	0.01	18.88	0.01
10	14:39:35.910	-55:01:29.44	23.68	0.02	22.14	0.01	20.49	0.01

Table 1: Position and  $B$ ,  $V$  and  $I$  magnitudes (with relative errors) of ten stars around the companion to PSR J1439-5501. The ★ marks the identified companion.